ELSEVIER

Physics of the Earth and Planetary Interiors 102 (1997) 21–32

PHYSICS OF THE EARTH AND PLANETARY INTERIORS

On ACH, or how reliable is regional teleseismic delay time tomography?

F. Masson *, J. Trampert [1]

CNRS URA 1358— Ecole et Observatoire de Physique du Globe, 5 Rue René Descartes, 67084 Strasbourg Cedex, France

Received 16 October 1996; accepted 24 January 1997

Abstract

ACH (named after Aki et al., 1976, Bull. Seismol. Soc. Am., 66: 501–524; Aki et al., 1977, J. Geophys. Res., 82: 277–296) is a standard, widely used, method for three-dimensional seismic imaging of the Earth. The fundamental hypothesis which underlies the method is that the time residuals generated outside the given target volume (from the seismic source to the bottom of the modelled zone) are approximately constant across the seismic array. The main purpose of this study is to check this assumption. We computed travel times for a given station and event distribution using a three-dimensional global Earth model taken from seismic tomography. We found that the relative residuals generated outside the target volume are not negligible and that the fundamental hypothesis underlying ACH is thus not verified. These deviations are generated in the lower and/or upper mantle and the corresponding proportions are entirely dependent on the raypaths. The bias in the inverted model is statistically similar to the input model outside the target volume. We thus recommend caution in any interpretations involving ACH-generated models. A secondary, somewhat independent, outcome of this study is that Fermat's principle, used to linearise the inverse problem in ray theory based tomography, seems to be valid without any restrictions (given our input model is representative for the true Earth) for rays with turning points in the lower mantle. For rays with turning points in the upper mantle, the constant raypath approximation is probably not true. This applies to global tomography as well. ©1997 Elsevier Science B.V. © 1997 Elsevier Science B.V.

1. Introduction

The oldest method for three-dimensional seismic imaging of the Earth's internal structure is the so-called 'ACH method' named after Aki et al. (1976, Aki et al., 1977). An excellent review of the method has been given by Evans and Achauer (1993), who described its mathematical formulation, reviewed the method's capabilities and limitations to retrieve some chosen 3-D structures and gave a very exhaustive bibliography of its different applications. The method applies to all seismic tomography problems in which the raypath is not entirely contained in the volume where the 3-D structure is sought. The final parts of upgoing rays are modelled in three dimensions whereas a standard Earth model is used outside this target volume. The method is mainly used for velocity imaging using teleseismic travel times, but has also found applications in attenuation and anisotropy modelling. Many research efforts have been made to

* Corresponding author, at: Geophysical Institute, University Karlsruhe, Hertzstr. 16, 76187 Karlsruhe, Germany e-mail:fmasson@9piwap1.physik.uni-karlsruhe.de.

[1] Present address: Department of Geophysics, University of Utrecht, P.O. Box 80021, 3508 TA Utrecht, Netherlands.

PII S0031-9201(97)00005-8

investigate the robustness of the method, concerning noise and outliers in the data, inhomogeneous datasets, different parameterisations of the target volume and diffraction effects. The enormous success of the method, according to Evans and Achauer (1993), may be attributed to the production of credible and geologically reasonable results from data that are widely available, easily obtained and handled at a relatively low cost. However, as Aki (1993) interestingly pointed out: "the issue of believability will haunt seismic tomography as long as subjective elements are needed in characterising the model structure and choosing the a priori stochastic properties of the model". This brings us to the fundamental hypothesis which underlies the ACH method and which to our knowledge has never been fully investigated: namely, the implicit correction of what happens to the raypath outside the target volume. In what follows, we will only concentrate on teleseismic travel time tomography. Here, the part outside the volume to be investigated is modelled by a standard 1-D velocity model. Residuals are contaminated by hypocentre and origin time errors and by differences between the average and true Earth model outside the target volume. Given the distance between source and receivers, together with diffractive healing of the wavefront (Wieland, 1987), it is commonly assumed that these errors are nearly constant for one source across the array. If these errors are indeed constant, they may be removed by forming relative residuals. Attempts have been made to see what happens to the resulting models if perturbations are put just underneath the target volume by Evans and Achauer (1993), who found that only the bottom layers of the target volume, where the resolution is lowest, are affected. We propose to fully investigate the fundamental hypothesis underlying ACH, which states that the errors for one given source are relatively constant through the receiver array. We generated synthetic arrival times in a 3-D earth taken from global tomography. This model should be understood as being our known Earth, and conclusions concerning the real Earth are only valid as far as the chosen global tomography model is a fair representation of the real Earth. Many scientists have noticed that structures seen by global and regional tomography differ. Although this is an interesting debate, our study is not intended to address this problem. The global seismic tomography model merely acts as an input to generate realistic data for an ACH inversion. The source and array distributions are taken from a real ACH experiment and the arrival times are treated in exactly the same manner as real data. The differences between the final result and the input model are a direct indication of the validity of the ACH fundamental hypothesis.

2. Experiment

We simulated a real situation of teleseismic travel time tomography, taking an existing 3-D Earth model in which we calculated travel times, based on the geometry of an existing ACH case. We analysed the residuals in strictly the same manner as done with real data. Because the result is known in our experiment, we can draw immediate conclusions as to the contamination of the target volume by the 3-D structure outside.

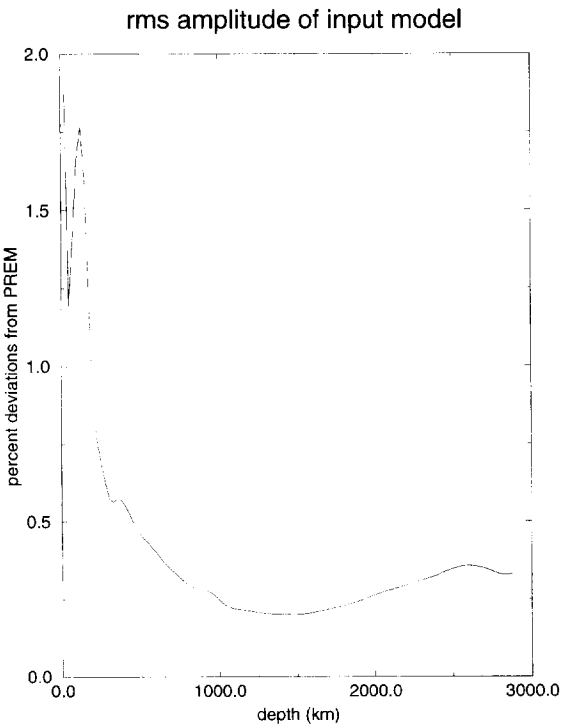

Fig. 1. The r.m.s. amplitude as a function of depth of the input model. Velocity perturbations are given in per cent with respect to PREM.

Since the early 3-D models of the beginning of the 1980s, essentially based upon long period surface waves (Woodhouse and Dziewonski, 1984) or ISC travel times (Dziewonski, 1984), efforts have been made to increase lateral resolution (e.g. Zhang and Tanimoto, 1993) and vertical resolution (e.g. Su et al., 1994). A new generation of models (e.g. Woodhouse and Trampert, 1997) based upon much shorter period phase velocity maps derived from tens of thousands of measurements and many body waveforms, have unprecedented lateral (1000–1600 km) and vertical (50–70 km in the upper mantle) resolution over the whole globe and show new features in the uppermost mantle. In our simulations, we will use such a model, expressed in S-velocity perturbations with respect to PREM (Preliminary Reference Earth Model; Dziewonski and Anderson, 1981). We converted the original shear wave to compressional wave velocity perturbations assuming the scaling relation $d\log V_s / d\log V_p = 2.0$ derived from travel time residuals (e.g. Souriau and Woodhouse, 1985). As we will show below, this scaling has no bearing on the conclusions drawn from our results. The r.m.s. amplitude vs. depth of our input model is shown in Fig. 1. Its main feature is that the most important anomalies are concentrated in the first 200 km. Travel times are calculated with a finite difference method developed by Podvin and Lecomte

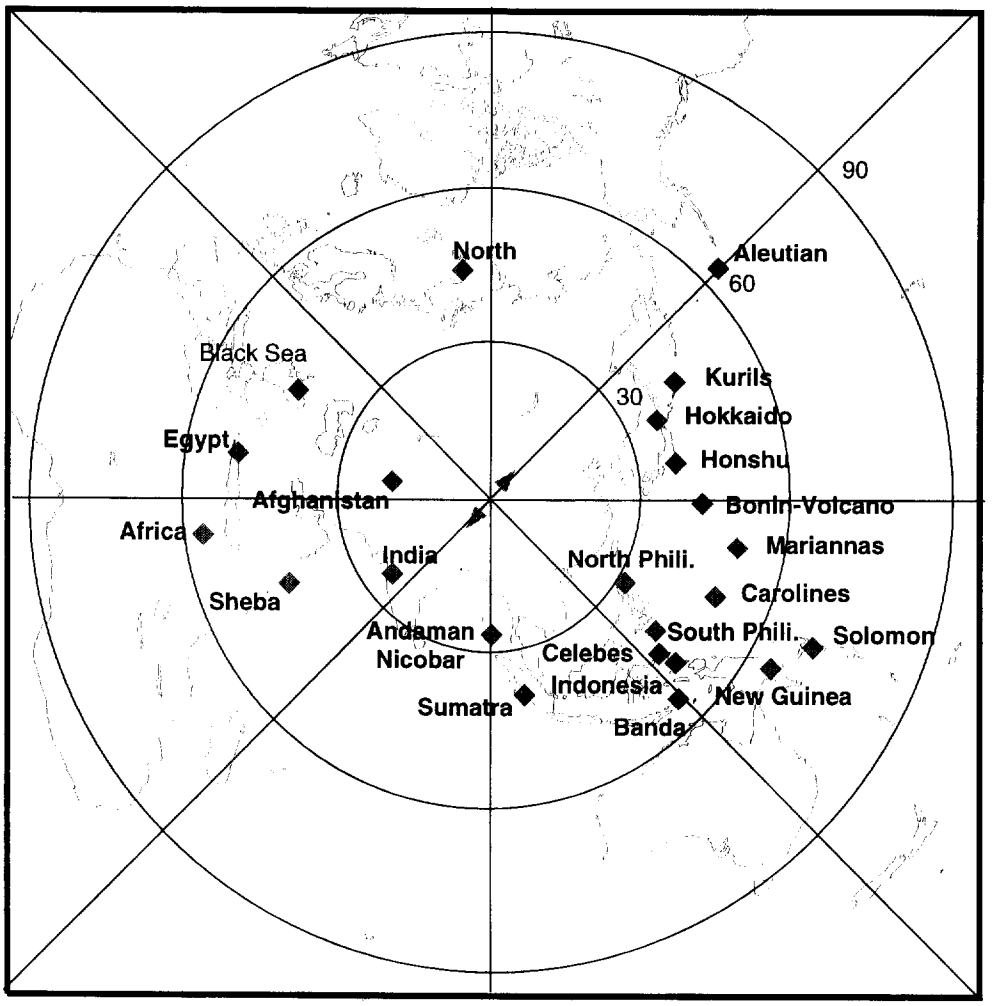

Fig. 2. Azimuthal equidistant map of epicentres used in this study. The location of the network is marked by a couple of arrows.

(1991). The model space is discretised on a grid. Every grid point is associated with a velocity value. A source is placed at a point of the model space (not necessarily at a grid point) and a wave front is propagated through the grid. The arrival times at any point of the model space are obtained by interpolation. We thus obtain the travel time of the first arriving wave in a 3-D Earth. The station distribution has been borrowed from a real teleseismic tomography experiment in northern Tibet described by Wittlinger et al. (1996). Their linear array consisted of 50 stations with a total length of about 600 km. They used data from 124 earthquakes, but the azimuthal coverage was still uneven so that they had to perform synthetic tests with 23 events to check for possible biases. We used these 23 events (Fig. 2) to generate 1150 arrival times in our 3-D earth model. The details of the events are given in Table 1. The PREM arrival times have been calculated in exactly the same manner, which gives us consistent time residuals for all raypaths.

After a detailed discussion of the obtained residuals, we invert these data using the same parameters as Wittlinger et al. (1996). The inversion is done to a depth of 400 km, which corresponds to two-thirds of the extension of the array. This rule-of-thumb is often used in such studies and seems to give optimum results (Evans and Achauer, 1993). Although we are following the same steps as Wittlinger et al. (1996), this work is not intended to verify or falsify their results; we simply needed a realistic ACH experiment to perform our study.

Table 1
Location and epicentral distances of the teleseismic events used in this study

Location	Latitude	Longitude	Epicentral distance
Honshu	34.351	139.711	37.3
Bonin	25.563	141.499	41.8
Egypt	28.624	34.588	50.1
Indonesia	−0.018	128.711	47.9
Kuriles	46.641	150.096	43.0
Marianas	15.670	144.951	49.5
Banda	−6.584	128.519	52.9
Celebes	2.339	125.911	44.3
Carolines	9.214	138.224	48.0
Solomon	−5.657	153.597	69.3
Hokkaido	42.818	140.451	36.5
New Guinea	−6.175	145.602	63.8
N. Philippines	16.604	121.600	31.0
S. Philippines	6.600	125.822	41.0
Sheba	12.429	54.352	42.4
Black Sea	43.702	37.997	43.2
Sumatra	−2.033	100.635	37.8
North	78.634	65.192	45.0
Africa	13.449	35.660	56.5
Aleutian	51.663	−175.212	63.7
India	19.383	74.093	23.7
Afghanistan	36.456	69.891	19.5
Andaman	9.518	94.564	25.8

3. Residual analyses

All calculated residuals between the source and the base of the target volume are shown in Fig. 3. The name of the event is marked on top of each individual plot and refers to the names shown in Fig. 2. The residuals presented as a function of station number have been subtracted by their mean residual through the network. We have chosen to show the residual curves up to the bottom of the target zone only, so that the fact that they are not flat is a direct indication that the fundamental hypothesis of the ACH method is generally not verified. The obvious questions are then how important is this deviation and are there any general trends which might allow us to infer which part of the Earth causes the strongest deviations.

The relative residuals of Fig. 3 are generally small (less than 0.2 s). Although they are certainly an order of magnitude smaller than those of Wittlinger et al. (1996) for instance, studies have been published with relative residuals of the same order as those of Fig. 3 (e.g. Iyer and Hirahara, 1993). Anyhow, the amplitudes of the residuals are directly dependent on the amplitude of the input velocity model and, as we will show below, behave almost linearly with the input model. Our model is long wavelength (roughly 1000 km horizontally) and has a relatively low r.m.s. amplitude as a function of depth (Fig. 1). We thus expect the effects shown to be conservative estimates.

The observed relative residual curves cannot be explained by effects such as different depth penetrations of rays or dipping layers. The only general trend one might wish to point out is that residuals for waves approaching from the west are generally

stronger. The question is then where these residuals are generated—in the upper mantle where our Earth model presents smaller-scale heterogeneities but high velocity contrasts, or in the lower mantle where we have large-scale heterogeneities but low velocity contrasts? To check this point, we partitioned our model into two separated models in which we computed all residuals again. The first model (UM) is constructed from the heterogeneities of the upper mantle only; the lower mantle is taken spherically symmetric and corresponds to PREM. The second model (LM), on the other hand, is constructed from the lower mantle of Woodhouse and Trampert (1997) and PREM in the upper mantle. All residuals corresponding to our 23 events are shown in Fig. 4; this time they include the target zone to be inverted for as well. The difference between the total residuals in Fig. 4 and the residuals in Fig. 3 comes, of course, from the contribution of the target zone, where our input model is not homogeneous. The reader may easily convince himself by considering the cross-section of the input model shown at the top of Fig. 6 (see below). Roughly, below Stations 1–25 (from the NE) the input model is slow, whereas it is fast below Stations 26–50 (towards the SW). For events lying in the azimuth of the network, residuals observed at

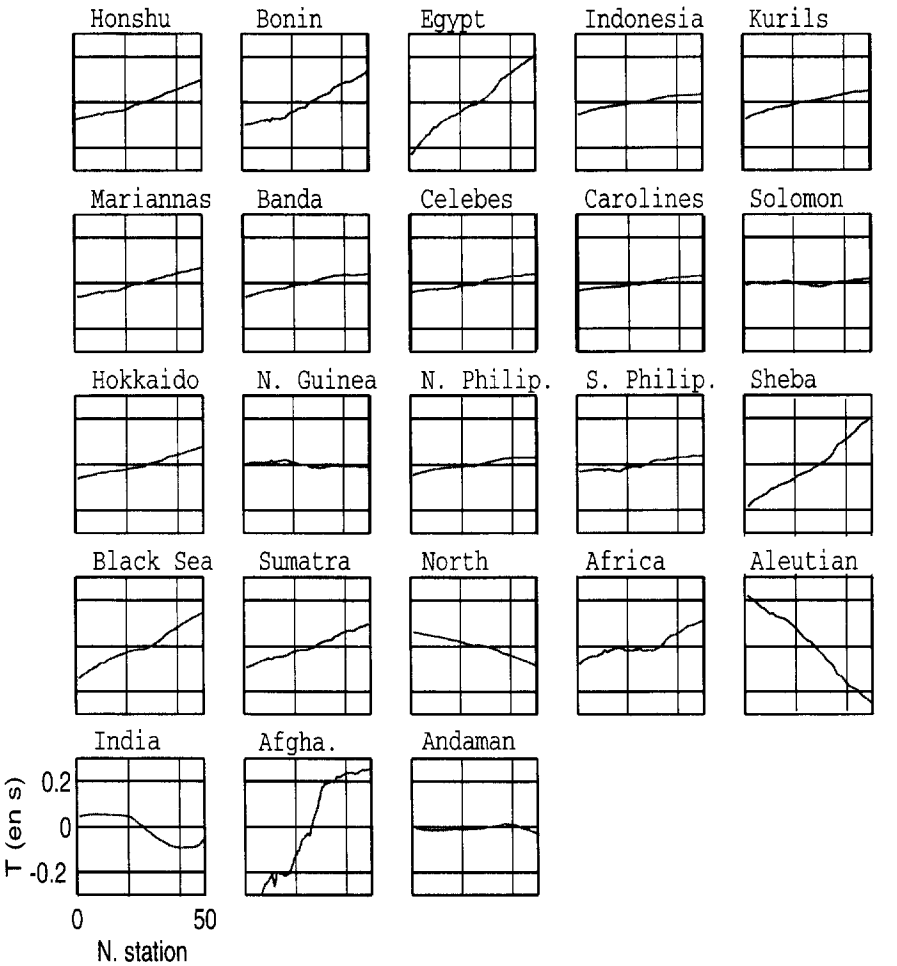

Fig. 3. Residuals with respect to PREM calculated for the 3-D velocity input model between source and base of the target volume. The residuals are subtracted by their mean residual through the network. They are plotted as a function of station number (Station 1 in NE, Station 50 in SW).

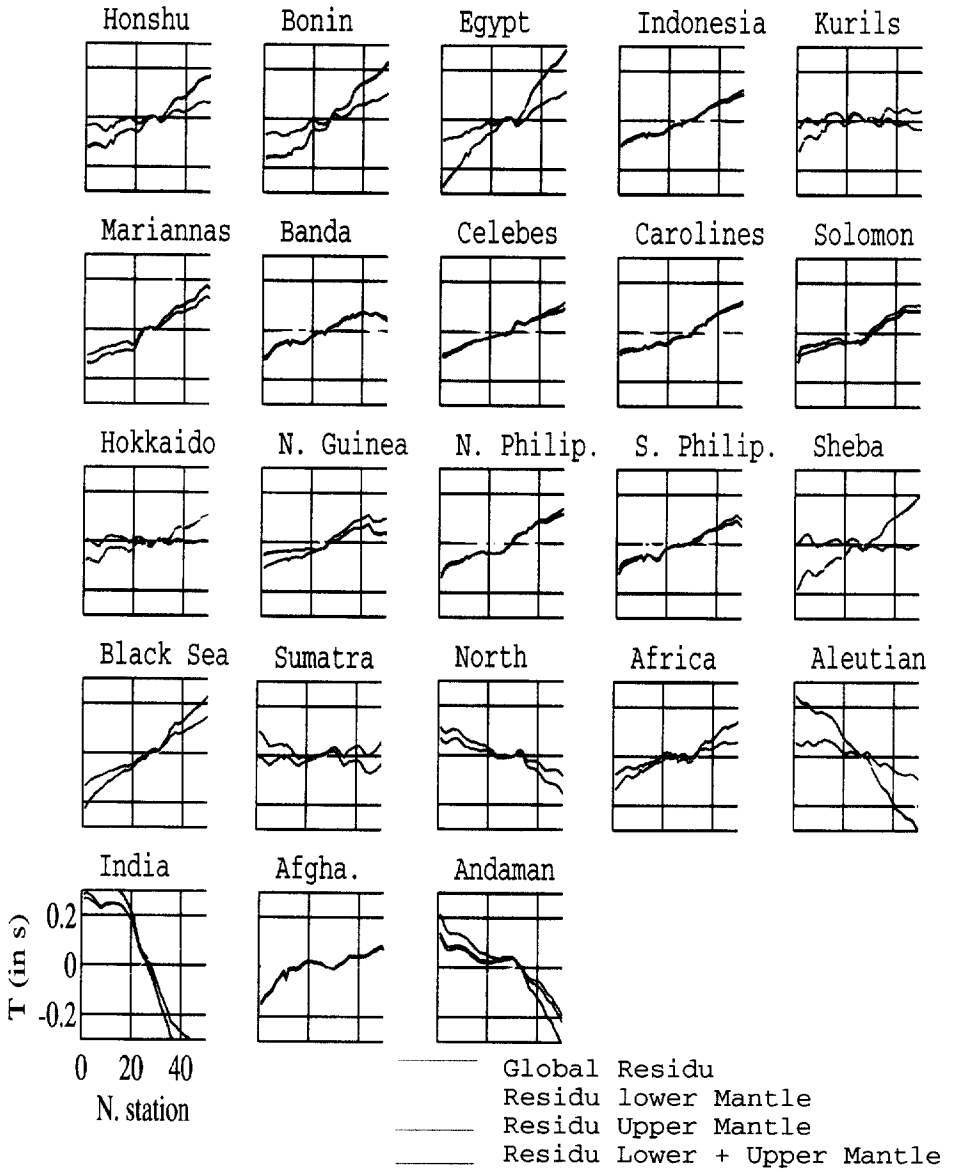

Fig. 4. Same as Fig. 3 between source and stations including target zone with: red line, total residuals calculated for the 3-D velocity input model; yellow line, residuals calculated for the lower-mantle (LM) model; green line, residuals calculated for the upper-mantle (UM) model; blue line, sum of the lower-mantle model and upper-mantle model residuals.

Stations 1–25 should then obtain a positive contribution from the input model in the target zone, whereas the opposite should apply for Stations 26–50. For events from the Aleutians and India this is exactly what is observed. For other events, 3-D effects of the input model have to be taken into account, and Fig. 6 is not sufficient to explain the observed differences.

In some cases the residuals can almost completely be attributed to LM residuals (e.g. Sheba), in other cases entirely to UM residuals (e.g. Banda), or a mixture of the two. The residuals computed across the LM model are smoother compared with the UM residuals. This can be explained by the variation of the wavelength of the heterogeneities vs. depth. The

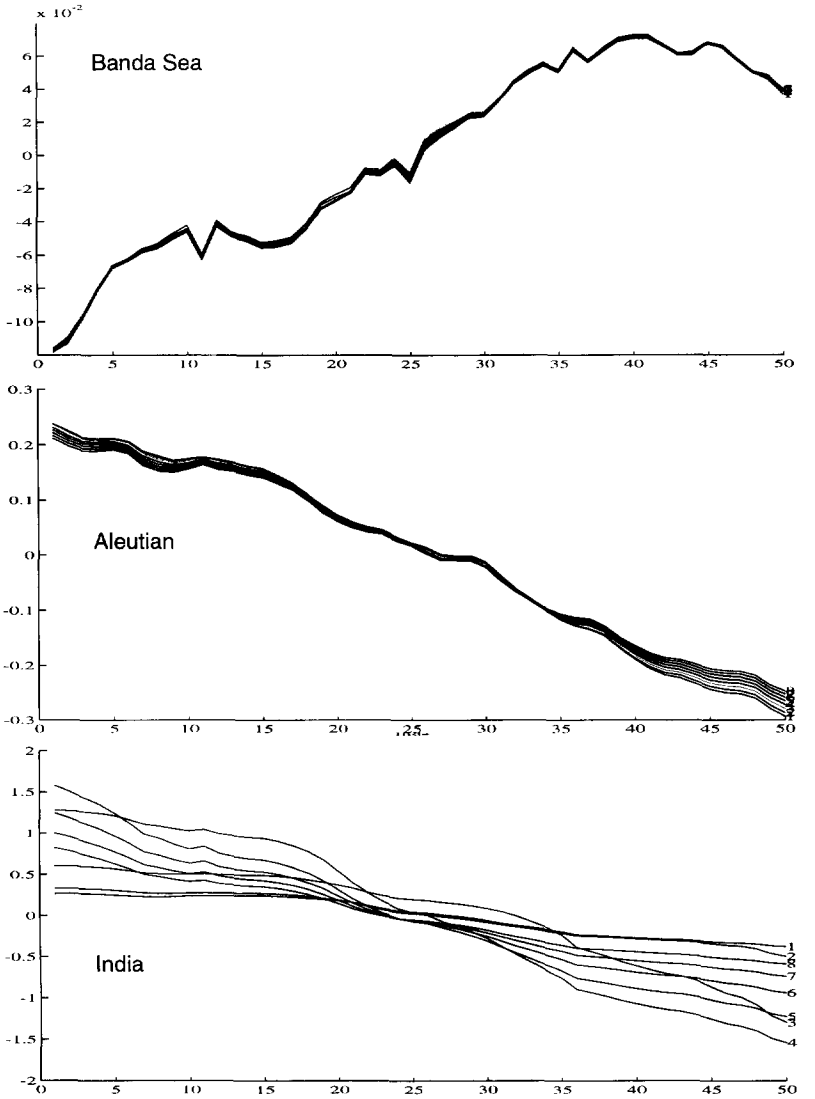

Fig. 5. Residuals generated for the whole Earth model multiplied by a factor varying between two and eight. The computed residuals for the model multiplied by n have been divided by n to allow a direct comparison with the original residuals.

amplitudes of the LM model and the UM model residuals are comparable, and it is not possible to say whether the residuals are mainly generated by the UM or the LM model. Only the events located near the array are obviously exclusively affected by the UM model because corresponding rays hardly touch the lower mantle. To summarise, the residuals of the lower mantle alone are generally not negligible compared with the upper-mantle ones.

Another interesting feature in Fig. 4, independent of our initial problem, is that the sum of the UM and LM residuals equals the residuals across the whole model. This is true for all the events and shows the linearity between travel time residuals and velocity perturbations. The reader is, of course, not surprised to see that Fermat's principle or the constant raypath approximation is verified for our input model, which is weak, as discussed above. We wanted to investigate this linear behaviour further, and computed residuals for input velocity perturbations which were

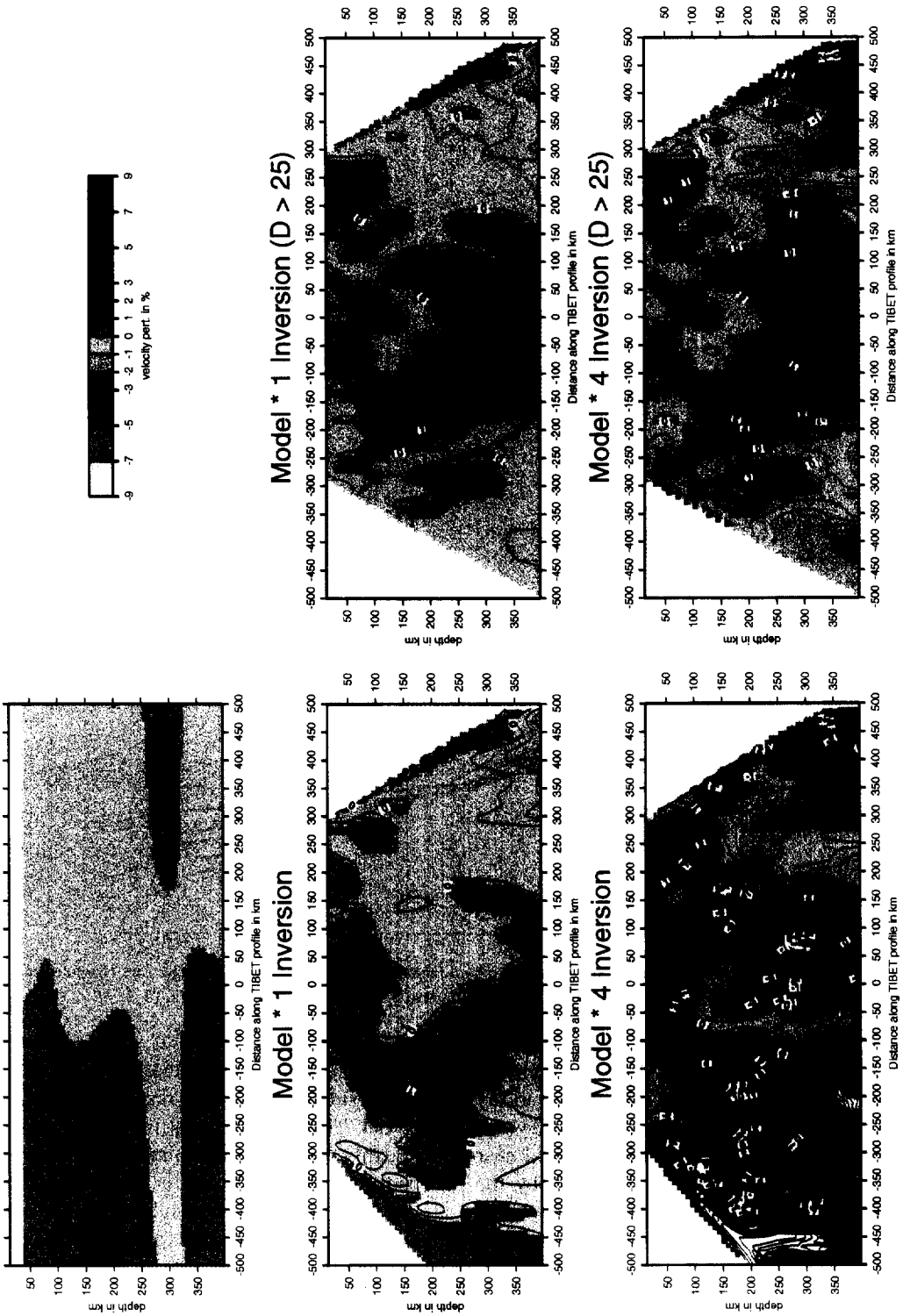

Fig. 6. Top: input model in the target zone (left side SW); middle, models obtained by inversion of the residuals computed for the input model (left, using the whole data set; right, using events with an epicentral distance greater than 25°); bottom, same as middle but using the input model multiplied by four.

multiplied by factors varying between two and eight. To fix ideas, for a factor of eight, velocity perturbations may reach 50% in parts of the upper mantle! Some whole Earth residuals are shown in Fig. 5. The computed residuals across the model multiplied by n have been divided by n, to allow a direct comparison with the residuals computed across the original model. Two examples of far events (Banda Sea and Aleutians) are shown for which the raypaths follow Fermat's principle perfectly. We notice that the constant raypath approximation does not depend on whether the main contribution of the residuals comes from the UM or LM. The raypaths corresponding to the three nearest events (India, Afghanistan and Andamans) do not show any linearity. The non-linearity starts to appear when upper mantle heterogeneities reach approximately 15%, which are values we can easily conceive for the real Earth. This is probably due to the fact that these rays have their turning points in the upper mantle, where the heterogeneities are strongest. These rays are most sensitive to vertically varying structure, and our input model has a very good vertical resolution (50–70 km) in the upper mantle. For the more distant events, upper-mantle paths are close to the vertical and less deviated. These rays are most sensitive to horizontally varying structure, and the horizontal wavelength of our input model is larger than 1000 km.

4. Inversion

ACH is based on a linear inversion to map the observations into the target volume. We should thus expect similar results to those observed in the data space regarding falsification of the fundamental hypotheses and linearity. Still, it is useful to quantify effects in the model space. We first inverted the residuals computed across the input model using our 23 events and then we inverted only the events with a epicentral distance greater than 25° (20 events). This leaves out data corresponding to the three nearest events (India, Afghanistan and Andamans). A cut-off distance of 25° is often used as rule-of-thumb in ACH inversions (Evans and Achauer, 1993). The resulting models are shown in Fig. 6. Our input model has a horizontal wavelength of more than 1000 km in the target zone. The vertical wavelength of the input model is of the order of the block size, but ACH, because of the use of relative residuals, cannot detect this variation. As a result, the input model seen through ACH has hardly any signal at all (Fig. 6, top). The inversion of the total residuals of Fig. 4 gives the models shown in Fig. 6 (middle). The maximum amplitude of the inverted anomalies is about 1% and the r.m.s. amplitude is about 0.5%, which is comparable with the r.m.s. amplitude of the input model. However, the shape of the anomalies is completely different. The input model has predominantly horizontal features, whereas the inverted model has predominantly vertical features which are a first indication of smearing along the raypaths. Leaving the closest events out in the reconstruction gives a slightly different model. This can be explained by the omission of raypaths in the southern part of the target zone. As a result, the heterogeneities (especially the positive anomaly) closely follow the vertical rays, indicating a more important smearing. The reader might argue that for these small amplitudes there is not really a problem, as normally small amplitude heterogeneities are not subject to interpretation. But what happens if we invert the data computed for the input model multiplied by factors of 2–8 (see previous section)? The results obtained using a factor of four are displayed in Fig. 6 (bottom). We immediately see that the retrieved model shows higher amplitudes when the velocities of the input model increase. If we invert all data, the final model shows strong signs of non-linearity. This is due to the fact that we included data for which Fermat's principle was violated. Not only do we import signal from outside the target zone into the model, but we also include non-linear effects because the argument which has been used to linearise the problem is no longer valid. If we respect the minimum epicentral distance criterion of 25°, the final model again behaves linearly with input. In this case, we retrieve the velocity model obtained for the first inversion, simply multiplied by the coefficient used to scale the input model. The smearing along the raypath now becomes very obvious. Statistically, the inverted model (obtained by respecting the distance criterion) is comparable with the input model outside the target zone, which indicates that the outside model leaks into the target zone preserving r.m.s. amplitude. This can be seen in Fig. 7, where

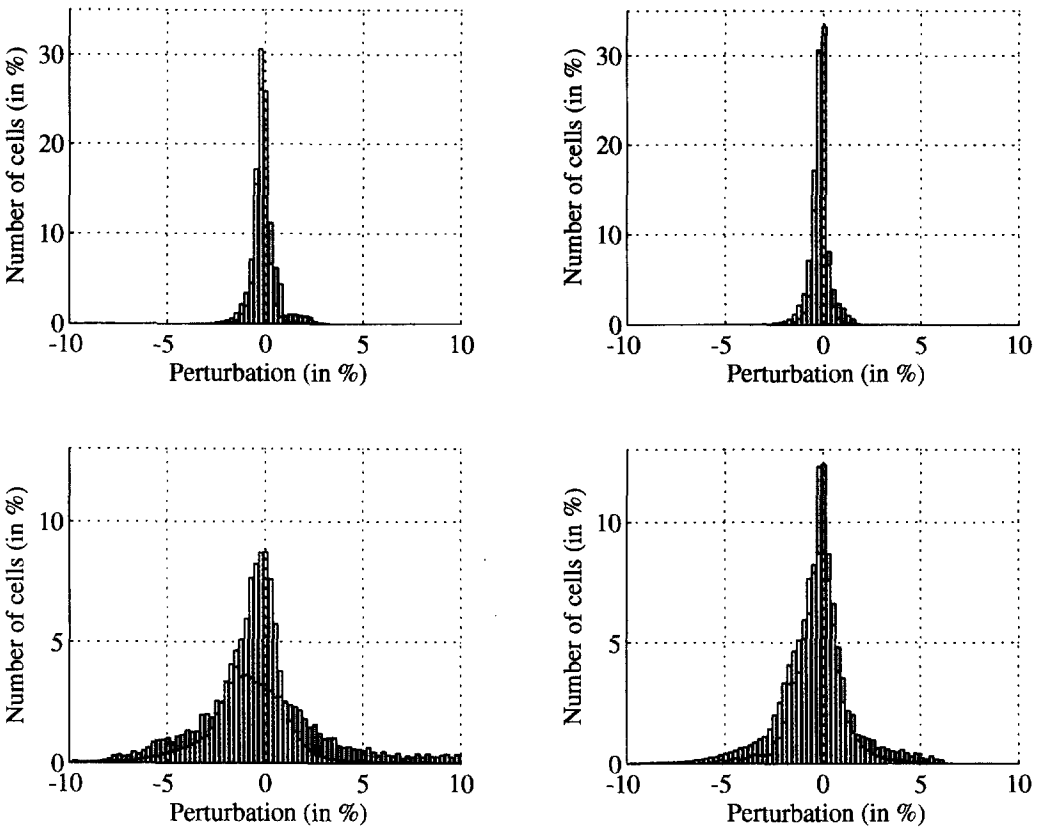

Fig. 7. Top: histograms of input heterogeneities counted on the grid for the whole Earth model (red) and inverted model heterogeneities counted in the target zone (blue) only (left, using the whole set of data; right, using the events with a epicentral distance greater than 25°). Bottom: same as top but using the input model multiplied by four.

we show histograms of input heterogeneities counted at the grid points of the whole Earth model and inverted models counted in the target zone only.

5. Discussion

If the true Earth resembles the Earth model of Woodhouse and Trampert (1997), then the ACH fundamental hypothesis is not verified and heterogeneities from outside the target zone leak into the target zone with similar amplitude. If, furthermore, the P-velocity amplitudes inferred from the S-wave model of Woodhouse and Trampert (1997) are representative of the true Earth, Fermat's principle is valid for all epicentral distances and the leakage is rather small in amplitude. In this case, ACH models can be regarded as significant with an amplitude larger than approximately 2% (to be on the safe side). If the input amplitudes, however, have been underestimated, Fermat's principle quickly breaks down for epicentral distances shorter than 25°. Leakage becomes more important and makes the interpretation of the ACH model more difficult. Anomalies aligned along the raypaths might be an indication, but of course heterogeneities from inside the target volume also smear out along the paths owing to bad resolution. If the true Earth has heterogeneities with shorter wavelengths than those used here, as has been suggested by Gudmundsson et al. (1990) and Snieder et al. (1991), the effects should be worse.

What can be done? We mainly see two remedies. The first approach would consist of modelling the residuals for a given seismic source to the bottom of

the target volume. In the classical ACH method, this residual curve is assumed to be flat and eliminated from the equations by forming relative residuals (see Evans and Achauer (1993) for details). Looking at Fig. 3, all residual curves could be modelled by polynomials up to degree three. In addition to the blocks forming the target volume, we would have to invert for four additional parameters per seismic source. This is similar to classical velocity and hypocentre determinations, with all the drawbacks of trade-off and increased model space. In other cases, a degree three polynomial might not be sufficient. For 2-D arrays, the residuals outside the target volume would need to be described by a more or less complicated surface. The advantage would be that working with absolute residuals would now make it easier to interpret depth profiles. The second approach is inspired from the leakage properties of truncated model spaces described by Trampert and Snieder (1996). The target volume and the rest of Earth can be regarded as complementary subspaces of the true model space. The data are built from these complementary parts outside and inside the target volume. It can be shown that if the sampling of the Earth is not homogeneous, which it never is, the part of the data up to the bottom of the target volume always has a projection into the model subspace spanning the target volume. Trampert and Snieder (1996) showed formally how to avoid this leakage. The Gram matrix for the ACH inversion (formed in this case from completely known partial derivatives) is readily calculated, and it might be worth investigating how this technique could effectively be used in the ACH case.

We have only investigated the situation corresponding to a linear array, but the last argument concerning the leakage of truncated model spaces will also apply to two-dimensional arrays, as the ray geometry outside the target volume will never be homogeneous. We thus strongly recommend that in all new ACH experiments the Earth outside the target volume is modelled, either explicitly or implicitly, because contaminations are unavoidable and make an interpretation of the inverted model extremely delicate.

A secondary outcome of this study relates to Fermat's principle. In global as well as regional tomography using delay times, rays are traced in a reference model. If, for the true Earth, deviations from the reference Earth are not too strong, Fermat's principle leads to errors in the raypath of second order. This is the central argument for use of linearised tomography, as it fixes the raypaths to those obtained in the reference model. We find that this is probably true for rays with turning points in the lower mantle. For rays with turning points in the upper mantle, the constant raypath approximation is probably not true.

References

Aki, K., 1993. Overview. In: H.M. Iyer and K. Hirahara (Editors), Seismic Tomography: Theory and Practice. Chapman and Hall, London, pp. 1–8.

Aki, K., Christofferson, A., Husebye, E.S., 1976. The three-dimensional seismic structure of the lithosphere under Montana LASA. Bull. Seismol. Soc. Am. 66, 501–524.

Aki, K., Christofferson, A., Husebye, E.S., 1977. Determination of the three-dimensional seismic structure of the lithosphere. J. Geophys. Res. 82, 277–296.

Dziewonski, A.M., 1984. Mapping the lower mantle: determination of lateral heterogeneity in P velocity up to degree and order 6. J. Geophys. Res. 89, 5929–5952.

Dziewonski, A.M., Anderson, D.L., 1981. Preliminary Reference Earth Model. Phys. Earth Planet. Inter. 25, 297–356.

Evans, J.R. and Achauer, U., 1993. Teleseismic velocity tomography using the ACH method: theory and application to continental-scale studies. In: H.M. Iyer and K. Hirahara (Editors), Seismic Tomography: Theory and Practice. Chapman and Hall, London, pp. 319–360.

Gudmundsson, O., Davies, J.H., Clayton, R.W., 1990. Stochastic analysis of global travel time data: mantle heterogeneity and random errors in the ISC data. Geophys. J. Int. 102, 25–43.

Iyer, H.M. and Hirahara, K., 1993. Seismic Tomography: Theory and Practice. Chapman and Hall, London, 842 pp.

Podvin, P., Lecomte, I., 1991. Finite difference computation of traveltime in very contrasted velocity models: a massively parallel approach and its associated tools. Geophys. J. Int. 105, 271–284.

Snieder, R., Beckers, J., Neele, F., 1991. The effect of small-scale structure on normal mode frequencies and global inversion. Geophys. Res. 96, 501–515.

Souriau, A., Woodhouse, J.H., 1985. A worldwide comparison of predicted S-wave delays from a three-dimensional upper mantle model with P-wave station corrections. Phys. Earth Planet. Inter. 39, 75–88.

Su, W., Woodward, R.L., Dziewonski, A.M., 1994. Degree 12 model of shear velocity heterogeneity in the mantle. J. Geophys. Res. 99, 6945–6980.

Trampert, J., Snieder, R., 1996. Model estimations biased by truncated expansions: possible artefacts in seismic tomography. Science 271, 1257–1260.

Wieland, E., 1987. On the validity of ray approximation interpreting delay times. In: G. Nolet (Editor), Seismic Tomography with Applications in Global Seismology and Exploration Geophysics. D. Reidel, Dordrecht, pp. 85–98.

Wittlinger, G., Masson, F., Poupinet, G., Tapponnier, P., Mei, J., Herquel, G., Guilbert, J., Achauer, U., Guanqi, X., Danian, S. and Lithoscope Kunlun Team, 1996. Seismic tomography of northern Tibet and Kunlun: evidence for crustal blocks and mantle velocity anomalies. Earth Planet. Sci. Lett., 139: 263–279.

Woodhouse, J.H., Dziewonski, A.M., 1984. Mapping the upper mantle: three dimensional modelling of Earth structure by inversion of seismic waveforms. J. Geophys. Res 89, 5953–5986.

Woodhouse, J.H., Trampert, J., 1997. New geodynamical constraints from seismic tomography. Earth Planet. Sci. Lett. submitted.

Zhang, Y.S., Tanimoto, T., 1993. High-resolution global upper mantle structure and plate tectonics. J. Geophys. Res. 98, 9739–9823.